MITSUBISHI ELECTRIC RESEARCH LABORATORIES
https://www.merl.com

Topological Data Analysis for Image-based Machine Learning: Application to Electric Motors

Wang, Bingnan; Talukder, Khaled; Sakamoto, Yusuke

TR2022-113 September 29, 2022

Abstract

Many finite-element simulations are required to fully evaluate the performance of a motor design candidate at different operating points. In this work, we investigate deep learning based surrogate modeling technique for motor design optimization to reduce simulations required. In particular, we introduce topological data analysis to electric machine design, which extracts topological features from motor design images for the training of machine learning models. We introduce the process of computing persistence homology and Betti sequences, which serve as vectorized input data for machine learning models. We propose two-channel deep learning models, with one convolutional network branch built for motor image data, and another multi-layer perceptron branch for Betti sequences. We show with numerical tests that two-channel models perform better in prediction accuracy and generalization capability compared with models without topological feature input. The results show that the proposed strategy is effective for image- based deep learning problems.

IEEE International Conference on Electrical Machines (ICEM) 2022

Mitsubishi Electric Research Laboratories, Inc.
201 Broadway, Cambridge, Massachusetts 02139

Topological Data Analysis for Image-based Machine Learning: Application to Electric Motors

Bingnan Wang, *Senior Member, IEEE*, AKM Khaled Ahsan Talukder, and Yusuke Sakamoto

***Abstract*—Many finite-element simulations are required to fully evaluate the performance of a motor design candidate at different operating points. In this work, we investigate deep learning based surrogate modeling technique for motor design optimization to reduce simulations required. In particular, we introduce topological data analysis to electric machine design, which extracts topological features from motor design images for the training of machine learning models. We introduce the process of computing persistence homology and Betti sequences, which serve as vectorized input data for machine learning models. We propose two-channel deep learning models, with one convolutional network branch built for motor image data, and another multi-layer perceptron branch for Betti sequences. We show with numerical tests that two-channel models perform better in prediction accuracy and generalization capability compared with models without topological feature input. The results show that the proposed strategy is effective for image-based deep learning problems.**

***Index Terms*—Design optimization, Electric Machines, Machine Learning, Persistence Diagram, Surrogate Model, Topological Data Analysis**

I. Design Optimization of Electric Machines

Electric machines are widely used in many applications including consumer appliances, industrial appliances, and transportation. Power dense, energy efficient, and cost effective electric machines are highly desirable across all these application domains. While electric machine technologies are well established, the ever increasing requirements for electric machines especially in new application fronts of the modern society, such as electric vehicles and aircraft, pose new challenges for electric machine design. While there are many aspects in improving the performance of electric machines including advanced materials and manufacturing technologies, the design optimization of electric machines is an effective tool that motor designers can utilize toward these design goals. Bramerdorfer *et al.* reviewed techniques to optimize electric machines in [1], Most of which use a parameterized geometry linked to population-based optimization algorithms, such as genetic algorithms (GA). However, parameterized geometry limits the design space since the components can only take shapes within the specified parameter range. Topology optimization, on the other hand, can overcome this limitation of parametric optimization by allowing a free form exploration of the design space. Recently, some topology optimization techniques have been adapted for the design optimization of electric machines [2]–[5].

For the accurate analysis of electric machine performances, finite-element method (FEM) based numerical simulations are utilized by motor designers. However, such simulations can be time-consuming, especially when many different operating points need to be evaluated for a design candidate. For the topology optimization of electric machines, the long simulation time poses even larger challenge, due to the expanded design space, and the much increased number of design candidates to be evaluated as compared with conventional parametric optimization. Therefore, it is desirable to seek for alternative modeling and analysis methods other than FEM that can make fast predictions to the motor performance at different operating points. Surrogate model based optimization has been investigated to speed up the process [6]. However, due to the highly nonlinear nature, it is difficult for a surrogate model to determine the machine efficiency at different locations of the efficiency map with respect to a design parameter.

Recently, data-driven approaches have been proposed to address the problem, by developing machine learning and deep learning models for the estimation of output performances of an electric machine that are conventionally derived from FEM simulations [7]–[10]. For motor optimization problems, the cross section of each motor design candidate is often described by a two-dimensional image, which is fed to the trained machine learning model, which quickly provides predictions to the desired performance metrics, such as average torque, torque ripple, and efficiency. While many machine learning and deep learning models can be utilized, such as support vector regression models, Gaussian process regression models, and multi-layer perceptrons (MLPs), convolutions neural networks (CNNs) have proven to be very effective for image analysis and recognition. Through the application of relevant filters in convolution layers, a CNN is capable of capturing the spatial and temporal dependencies in an image, performing improved fitting to the image dataset over conventional methods. Many deep learning models have been proposed based on CNN for various applications. Developed for image recognition and trained with ImageNet [11], very deep convolutional networks, such as VGGNet [12] and ResNet [13], have achieved superior classification accuracy. CNN based models have also been applied to facilitate electric machine optimization

B. Wang is with Mitsubishi Electric Research Laboratories (MERL), 201 Broadway, Cambridge, MA 02139 USA (email: bwang@merl.com)

A. Talukder is with Department of Computer Science and Engineering, Michigan State University, East Lansing, MI, USA

Y. Sakamoto is with Advanced R&D Center, Mitsubishi Electric Corporation, Amagasaki, Japan

A. Talukder's work is done during his internship at MERL in 2021.

problems [7]–[10]. However, deep networks often have a huge number of parameters, in the order of millions, which require a large amount of data to train. In addition, they are susceptible to noisy data and tend to overfit with training data, and can have difficulty in generalizing over unseen data. Recently, transfer learning technique is applied to reduce the amount of training data needed, which adapts a VGG16 network pre-trained on ImageNet to the cross section images of electric motors, and tunes only a small part of the network for the prediction of motor performance metrics including average torque and torque ripple [14]. This is advantageous in reducing the amount of training data and the effort of retraining the network, as the model weights have already been trained on a huge dataset in ImageNet, which includes over 1.2 million images [11]. While one main advantage of CNN based network is the capability of extract features automatically through the training process, it falls short in the explainability as to what features are exactly learned, and the generalization capability to unseen data.

Topological data analysis (TDA), on the other hand, offers a mathematically rigorous way of extracting the shape information, or topological features of the data. Topology is a branch of mathematics to deal with qualitative geometric information [15], which studies the connected components of a space, such as the classification of loops and higher dimensional surfaces within the space. Compared with other straightforward geometric methods, which quantitatively describe geometric properties such as curvatures, topology describes geometric properties in a much less sensitive way to the choice of metrics. Topology is coordinate-free, and only extract intrinsic geometric properties of geometric objects. These features are attractive for addressing the challenges in many data analysis problems, such as the extraction of information from high-dimensional, incomplete, and often noisy datasets. Therefore, TDA, which develops and utilizes topological methods in data analysis, has been emerging in recent years, and seen applications in image analysis [16], time-series data analysis [17], sensor networks [18], chemistry [19], and material science [20], etc.

In this work, we explore TDA for deep learning based models for electric machine analysis and design optimization. We extract topological features, in particular, persistence diagrams and Betti sequences, from cross section images of electric machine design candidates, and together with the cross section images, to train a deep learning model for the prediction of two-dimensional flux map of a motor design. In particular, a multi-channel architecture is utilized for the deep learning model, with images fed into one branch of CNN based model, topological features extracted from the images fed into the other branch of MLP model, and the output of the two branches is then fed into a common set of dense layers before finally connecting to the flux map parameters to be calculated. We show that the prediction accuracy using topological features combined with cross section images is consistently better compared with models using motor cross section images only, indicating that the model generalizes better with unseen data with TDA.

The rest of the paper is organized as follows. In Section II we define the multi-output regression problem in motor analysis; in Section III, we introduce persistence homology and Betti sequence, the calculation process, and the analysis of obtained Betti sequences from motor images; in Section IV, we introduce the proposed deep learning model architecture and the set up of the training process; in Section V, we present the results of the numerical tests and discuss the effectiveness of the proposed method; in Section VI we conclude the paper.

II. Problem Definition

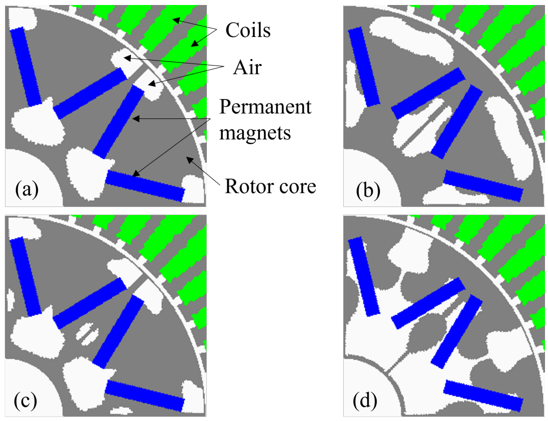

Figure 1. The cross-section image of an interior permanent magnet motor for the study.

In this study, we deal with the design optimization of an interior permanent magnet synchronous motor (IPMSM). The motor has 48 slots in the stator, 8 poles in the rotor with V-shaped permanent magnets embedded , and the whole rotor core region is subject to optimization. During the optimization process using GA and Normalized Gaussian network (NGnet) method, which is described in details in Ref. [8], a total of 27,949 design candidates are generated and evaluated using FEM simulations. A quarter of the cross-section of these design candidates are stored in the form of RGB images, with size 224 $\times$ 224 $\times$ 3, a few examples of which are shown in Fig. 1. Across all the design candidates, all other design parameters are kept the same, except for the shape of rotor core region. These images are collected and served as input data of the dataset for machine learning purposes.

For each motor design, magneto-static simulations are conducted at 100 operating points of d-axis current I_d and q-axis current I_q. The magnetic flux linkage ϕ_d and ϕ_q are obtained in each condition, in order to construct the 2D flux maps $\phi_d(I_d, I_q)$ and $\phi_q(I_d, I_q)$. Such 2D flux maps can be approximated described using the quadratic functions:

$$\phi_q = \beta_{q0} i_d^2 + \beta_{q1} i_q^2 + \beta_{q2} i_d i_q + \beta_{q3} i_d + \beta_{q4} i_q + \beta_{q5}, \quad (1)$$

$$\phi_d = \beta_{d0} i_d^2 + \beta_{d1} i_q^2 + \beta_{d2} i_d i_q + \beta_{d3} i_d + \beta_{d4} i_q + \beta_{d5}. \quad (2)$$

The 12 coefficients, β_{q0} through β_{d5}, in the quadratic equations are obtained through least-square fitting of simulation results for each design, and stored in the form a 12×1 vector. Fig. 2 shows the comparison of the q-axis flux map constructed directly from the FEM simulations, and the one generated from the fitted quadratic function for one design candidate, which matches well with the original. These coefficients in the vector form serve as the output data of the dataset. The goal in this work is to develop machine learning models to have good prediction of the 12 flux map coefficients for a new design candidate, such that the normalized root-mean-square error (RMSE) between the prediction and the ground truth values is as small as possible.

With the flux map, motor torque can be calculated with $T(i_d, i_q) = \boldsymbol{\phi} \times \boldsymbol{i} = \phi_d i_q - \phi_q i_d$. In recent study [21], CNN models have been developed to learn such current-dependent torque characteristics of motors.

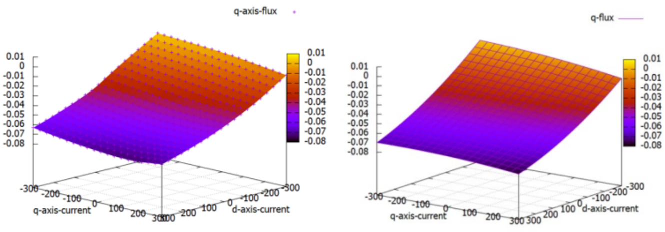

Figure 2. The comparison of q-axis flux map (a) obtained directly from FEM simulations, and (b) from fitted quadratic function.

III. Topological Feature Extraction

In this section, we give a brief introduction to topological data analysis method with persistent homology and the process of generating persistence diagram and Betti sequence from an input image, and discuss on the obtained Betti sequences from motor images.

Persistent homology is a powerful mathematical tool to compute the topological features of a space that persist across multiple scales. An important enabler for TDA, it is pioneered by Edelsbrunner [22], and Zomorodian and Carlsson [23], and gained popularity largely after the seminal paper by Carlsson in 2009 [15]. The key idea is to represent the data points (point clouds), sampled from the space, by a parameterized family of simplicial complexes. The homology of the data space can then be computed algorithmically through filtration of nested families of simplcial complexes, to not only obtain information about the topological features, but also encode their evolution across the scales, such as the birth and death of edges and holes.

A *simplicial complex* can be roughly considered as a union of points, edges, triangles, tetrahedrons, and polytopes in higher dimensions. A *filtration* of a simplicial complex K is a nested family of sub-complexes $(K_r)_{r \in T}$, where $T \subseteq \mathbb{R}$, such that for any r, $r' \in T$, if $r \leq r'$ then $K_r \subseteq K_{r'}$, and $K = \cup_{r \in T} K_r$ [24]. If $f : K \to \mathbb{R}$ is a function, then the family $K_r = f^{-1}((-\infty, r])$, $r \in \mathbb{R}$ defines a filtration called the sublevel set filtration of f.

In practice, the parameter r can be interpreted as the radius of the point clouds in the data. During the construction of filtration, some features may appear and then disappear and the *persistence* of these homological features can be considered as the features of the dataset. In a filtration, one can record the *birth*, which is the time a feature appears, and *death*, which is the time it disappears as it gets filled in with a lower dimensional simplex. The essence of the *persistent homology* is to track the birth and death of these homological features in $K = \cup_{r \in T} K_r$ for different r values, which can be described by a *persistence diagram*. A persistence diagram is a set of points $(b, d) | b, d \in \mathbb{R}^2$ and $d > b$, where each point corresponds to the birth and death of topological feature in a corresponding family of simplicial complexes. In particular, each point (b, d) denoted a topological features being born at radius b and "dying" at radius d.

There are different algorithms for the filtration of simplicial complexes and the computation of persistence diagrams, with implementations available by several software packages. In this study, we use the python library Ripser.py for the computation of persistence diagrams for all the rotor shapes [25].

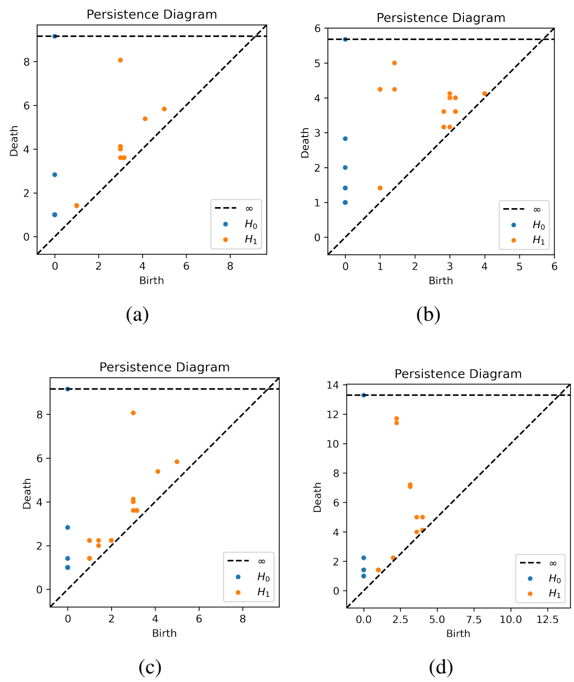

(a) (b) (c) (d)

Figure 3. Computed persistence diagrams for the four motor core designs shown in Fig. 1

There is a persistence diagram H_k for each homological dimension k, which can be combined into one single figure. Fig. 3 shows examples of computed persistence diagrams from the motor images corresponding those shown in Fig. 1, where both H_0 and H_1 diagrams are plotted. As can be seen, while these diagrams are distinct from each other, the number of points in a persistence diagram is not fixed for different input data. Since we want to use the topological features for machine learning purposes, and most machine learning models require input having the same length, we would hope to represent the persistence diagrams of different input data in a vectorized way. Betti sequence, or Betti curve, is an effective way to achieve that [24], [26]. A Betti sequence can be derived from a persistence digram. Assume D is a persistence diagram with a finite number of off-diagonal points, with $\alpha = (b_\alpha, d_\alpha)$ a point in the diagram, and maximum filtration radius $r_{max} > 0$, let $\{r_i\}_0^M$ be equally spaced points within $[0, r_{max}]$, the Betti sequence of D is a vector of length M defined as $\vec{\beta} = (\beta_i)_1^M$, with the entries β_i count the number of points in the persistence diagram at filtration radius r_i around the point clouds in the data space. In other words, if we define the function:

$$f_\alpha(r) = \begin{cases} 1, & b_\alpha \leq r \leq d_\alpha \\ 0, & \text{otherwise} \end{cases}$$

Then the points on a Betti sequence is obtained from the summation:

$$\beta_i = \sum_{\alpha \in D} f_\alpha(r_i).$$

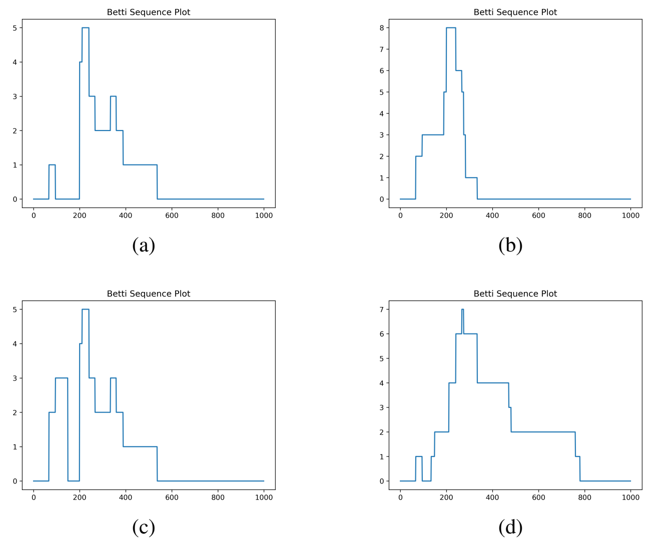

Figure 4. Computed Betti sequences for the four motor core designs shown in Fig. 1 and persistence diagrams shown in Fig. 3.

Fig. 4 show examples of computed Betti sequences from motor core images. In the computation all the Betti sequences have the same length of 1000, with the x-axis the index of the sequence corresponding to filtration radius, and y-axis the number of features corresponding to H_1 persistence homology. By comparing the figures we can see that the different rotor designs can be described by distinctive Betti curves.

IV. Network Architecture

In this study, a total of 12 flux map model coefficients needs to be determined for a given motor design image, which is essentially a multi-output regression problem. Many machine learning algorithms are developed for single-output regression, which predicts a single numeric value. While some algorithms do support multi-output regression, such as linear regression and decision trees, their performances for highly nonlinear problems with high-dimensional input data suffer. Deep neural network models are more commonly used to tackle such problems.

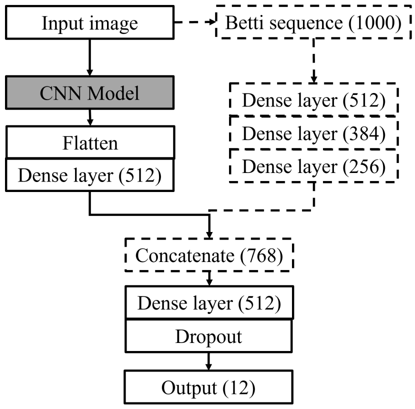

Figure 5. The high-level network architecture with input image and Betti sequences. When using only input image and CNN model, the steps with dashed lines are not implemented.

In this work, we propose a multi-channel architecture to utilize both the motor cross-section images and their extracted topological features represented as Betti sequences for the prediction of motor flux maps. The high-level structure is shown in Fig. 5, with the images fed into the first branch of deep convolutional network, while the corresponding Betti sequences fed into the second branch of MLP network. The output from the CNN model is flattened and connected to a fully-connected layer of 512 nodes. The outputs of the two branches are then concatenated together as the input of a subsequent fully-connected layer, before connecting to the output of 12 flux map coefficients. For comparison, when using only the cross-section images without Betti sequences, the second branch of the network (steps with dashed lines in the diagram) is removed, leaving only the CNN branch. For the Betti sequence branch, we vectorize the Betti sequences of all design images with the same length of 1000, and feed them into a MLP network of three dense layers of size 512, 384, and 256 nodes respectively.

For the CNN model structure, we tested two different approach: a simple vanilla CNN with two convolution layers, and a deeper model based on ResNet50 [27], which has 48 Convolution layers along with 2 Pooling layers, and their model structures are shown in Fig. 6(a) and 6(b) respectively. For the vanilla CNN model, we first extract the rotor shape from the provided RGB images and reduce the size to 56×56 as input for the following layers, which include two convolutional layers with number of filters 32 and 48 respectively, and subsequent MaxPooling layers for feature extraction and dimensionality reduction, as shown in Fig. 6(a).

The high-level architecture of the ResNet50 model is

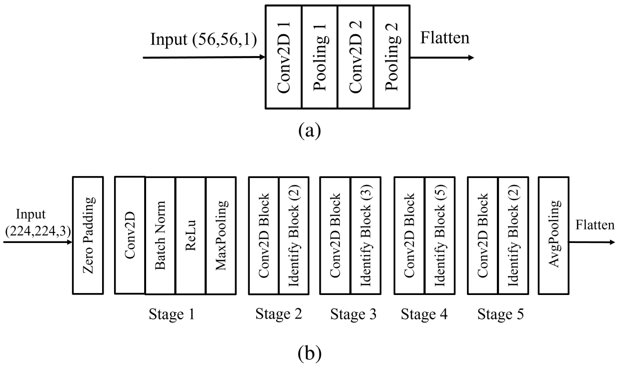

Figure 6. Two CNN models corresponding to the gray box in Fig. 5: (a) A vanilla CNN model; (b) ResNet50 model without subsequent dense layers. With transfer learning, trained weights from ImageNet are used, with only stage 4 and 5 weights retrained.

Table I
PARAMETERS FOR NUMERICAL TEST SETUP

Training data size	20124
Testing data size	7825
Traing/Testing split	72%/28%
Max. Number of epochs	200
Batch size	8

shown in Fig. 6(b). ResNet stands for residual network, which enables the effective training of very deep neural networks that were previously impossible to train due to vanishing gradients [27]. A key feature of ResNet is the "skip connections" in convolution blocks and identity blocks, which adds the input x itself to the output $\mathcal{F}(x)$ of each block including several convolution layers, so that the output becomes $\mathcal{F}(x) + x$. Skip connections set up a shortcut for gradients to pass through, which mitigates the vanishing gradient problem; they also allow the model to learn an identity function to ensure the higher layers perform at least as good as the lower layers.

For the ResNet50 model, we utilized two training method: training all model weights from scratch, and transfer learning with weights pre-trained from ImageNet. When transfer learning is utilized, we keep the model weights trained on ImageNet up to the third stage, and only retrain the later stages 4 and 5 using the motor dataset. Major parameters for the set up of the numerical tests are listed in Table I.

V. RESULTS AND DISCUSSIONS

With data pre-processed and deep learning models set up, we start the training process with each model. Due to the shuffling of data during the training, 3 independent tests are conducted for each model, and the convergence plots are shown in Fig. 7. For the vanilla CNN based models, as shown in Fig. 7(a), the two-channel model, which feeds the Betti sequences extracted from motor images into the second branch of MLP model, converges faster and performs better with lower root-mean-square error (RMSE), as compared with the single-channel model with CNN fed with motor images only. The ResNet50 based model achieves lower

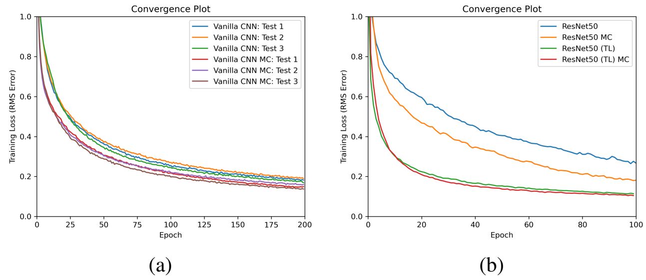

Figure 7. The convergence plot of the training process of each CNN model, and the corresponding multi-channel (MC) model with Betti sequences: (a) A vanilla CNN structure; (b) ResNet50 model trained from scratch, and with transfer learning (TL).

RMSE when trained from scratch using the motor dataset, and even better performance with transfer learning from ImageNet weights, as shown in Fig. 7(b). The training losses for the multi-channel (MC) models with Betti sequences included are consistently lower than their counterparts of models without Betti sequences.

We then test the trained models on the testing dataset, and the results are listed in Table II. For vanilla CNN, the MC model has a lower normalized RMSE of 0.297 in prediction for the 7825 testing data, as compared with 0.335 for single-channel model. For the ResNet50 models, the MC model has a lower RMSE of 0.242, as compared with 0.260 for the single-channel model when trained from scratch, both after 200 epochs of training. When transfer learning from ImageNet is utilized, the model achieves better performance with less number of epochs trained. The single-channel model has prediction RMSE 0.261 after just 50 epochs of training, and 0.218 after 100 epochs. With MC model, the RMSE is reduced to 0.255 after 50 epochs, and 0.214 after 100 epochs. The better results of deep ResNet50 based model show the improved feature extraction capability from images with more convolutional layers, and the effectiveness of transfer learning strategy [14]. The corresponding MC models with Betti sequences perform consistently better than CNN only models for making predictions on unseen data, which shows improved generalization capability. TDA provides a new tool for feature engineering of data structures, especially image data. Betti sequences extract topological features from the motor cross section images, and improve the effectiveness of the deep learning models.

To quantify the prediction error in more details, we plot in Fig. 8 and Fig. 9 the prediction of each flux map coefficient on all 7825 testing data, using the trained ResNet50 MC model, together with ground truth generated from FEM simulation. All coefficients agree very well with the ground truth values, with correlation coefficients higher than 0.96.

We want to mention that, while the training process takes hours, the prediction of the flux map using trained deep learning model is almost instantaneous for a given motor design. While the models were built for forward prediction in this work, deep learning models can also be built for the

Table II
FLUX MAP COEFFICIENTS PREDICTION PERFORMANCE ON UNSEEN TEST DATA USING VARIOUS TRAINED MODELS.
(TL: TRANSFER LEARNING. MC: MULTI-CHANNEL MODEL WITH BETTI SEQUENCES)

Model	Epochs trained	RMSE: Test 1	RMSE: Test 2	RMSE: Test 3	RMSE: Average
Vanilla CNN	200	0.335	0.349	0.320	0.335
Vanilla CNN MC	200	0.301	0.299	0.292	0.297
ResNet50	200	0.251	0.277	0.251	0.260
ResNet50 MC	200	0.240	0.243	0.243	0.242
ResNet50 (TL)	50	0.263	0.260	0.261	0.261
ResNet50 (TL) MC	50	0.256	0.257	0.252	0.255
ResNet50 (TL)	100	0.217	0.219	0.217	0.218
ResNet50 (TL) MC	100	0.216	0.217	0.210	0.214

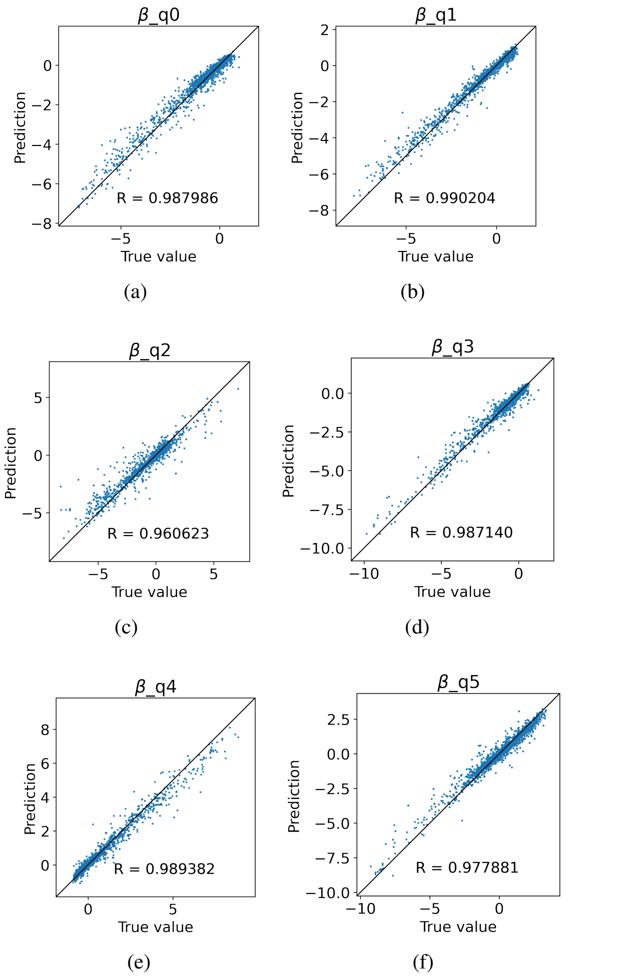

Figure 8. Correlation plot of the predicted flux map coefficients using ResNet50 two-channel model from β_{q0} through β_{q5}, with correlation coefficients between predicted value and ground truth listed for each plot.

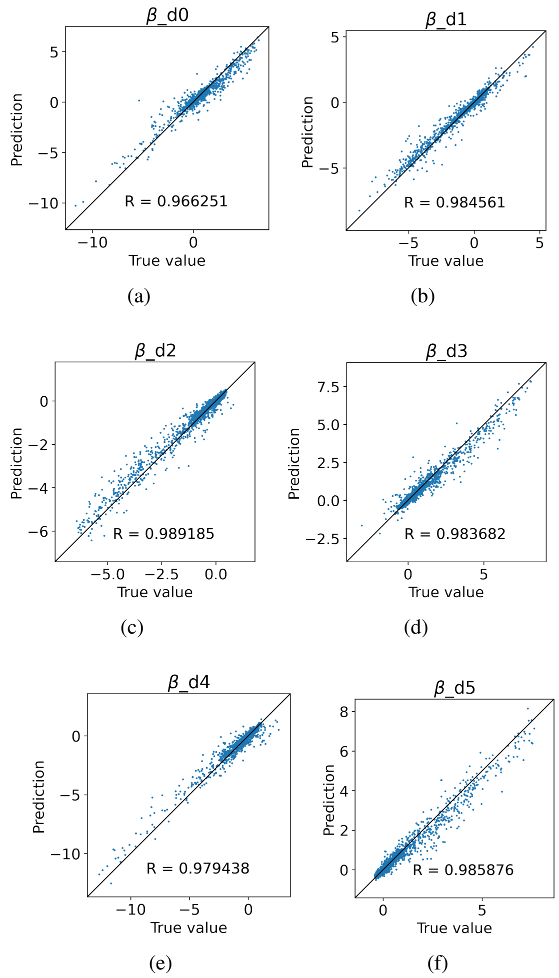

Figure 9. Correlation plot of the predicted flux map coefficients using ResNet50 two-channel model from β_{d0} through β_{d5}, with correlation coefficients between predicted value and ground truth listed for each plot.

inverse design of motors, to discover motor topology for given design objectives.

VI. CONCLUSIONS

In this work, we investigated the surrogate modeling technique using deep learning to facilitate the analysis and optimization of electric machines. Dozens of finite-element method based numerical simulations are typically required to obtain 2D flux map of a motor design under different operating points. The task is especially challenging when dealing with a large design space. We proposed to apply topological data analysis for the feature engineering of motor cross-section images, and use the vectorized Betti sequences obtained from the images for the training of deep learning models. Two-channel models with input data directly from the motor cross-section images and the computed Betti sequences were constructed. Compared with conventional CNN models using only the motor images, we show with numerical tests that the two-channel models with topological features in Betti sequences achieve lower RMSE and generalize better to unseen data. The effectiveness of the proposed method was validated with good accuracy in predicting the flux map coefficients. We expect the strategy of using vectorized topological features more broadly deployed to the feature engineering and image based deep learning applications.

VII. ACKNOLEDGEMENT

The authors sincerely thank Prof. Hajime Igarashi and Mr. Taiga Aoyagi from Graduate School of Information Science and Technology of Hokkaido University for the support of this work and generously providing the dataset.

REFERENCES

[1] G. Bramerdorfer, J. A. Tapia, J. J. Pyrhönen, and A. Cavagnino, "Modern electrical machine design optimization: Techniques, trends, and best practices," *IEEE Transactions on Industrial Electronics*, vol. 65, no. 10, pp. 7672–7684, 2018.

[2] T. Sato, K. Watanabe, and H. Igarashi, "Multimaterial topology optimization of electric machines based on normalized gaussian network," *IEEE transactions on magnetics*, vol. 51, no. 3, pp. 1–4, 2015.

[3] M. Garibaldi, C. Gerada, I. Ashcroft, and R. Hague, "Free-form design of electrical machine rotor cores for production using additive manufacturing," *Journal of Mechanical Design*, vol. 141, no. 7, 2019.

[4] A. Credo, G. Fabri, M. Villani, and M. Popescu, "Adopting the topology optimization in the design of high-speed synchronous reluctance motors for electric vehicles," *IEEE Transactions on Industry Applications*, vol. 56, no. 5, pp. 5429–5438, 2020.

[5] F. Guo and I. P. Brown, "Simultaneous magnetic and structural topology optimization of synchronous reluctance machine rotors," *IEEE Transactions on Magnetics*, vol. 56, no. 10, pp. 1–12, 2020.

[6] R. C. P. Silva, T. Rahman, M. H. Mohammadi, and D. A. Lowther, "Multiple operating points based optimization: Application to fractional slot concentrated winding electric motors," *IEEE Transactions on Industrial Electronics*, vol. 65, no. 2, pp. 1719–1727, 2017.

[7] S. Doi, H. Sasaki, and H. Igarashi, "Multi-objective topology optimization of rotating machines using deep learning," *IEEE transactions on magnetics*, vol. 55, no. 6, pp. 1–5, 2019.

[8] H. Sasaki and H. Igarashi, "Topology optimization accelerated by deep learning," *IEEE Transactions on Magnetics*, vol. 55, no. 6, pp. 1–5, 2019.

[9] A. Khan, V. Ghorbanian, and D. Lowther, "Deep learning for magnetic field estimation," *IEEE Transactions on Magnetics*, vol. 55, no. 6, pp. 1–4, 2019.

[10] A. Khan, M. H. Mohammadi, V. Ghorbanian, and D. Lowther, "Efficiency map prediction of motor drives using deep learning," *IEEE Transactions on Magnetics*, vol. 56, no. 3, pp. 1–4, 2020.

[11] O. Russakovsky, J. Deng, H. Su, J. Krause, S. Satheesh, S. Ma, Z. Huang, A. Karpathy, A. Khosla, M. Bernstein *et al.*, "Imagenet large scale visual recognition challenge," *International journal of computer vision*, vol. 115, no. 3, pp. 211–252, 2015.

[12] K. Simonyan and A. Zisserman, "Very deep convolutional networks for large-scale image recognition," *arXiv preprint arXiv:1409.1556*, 2014.

[13] K. He, X. Zhang, S. Ren, and J. Sun, "Deep residual learning for image recognition," in *Proceedings of the IEEE conference on computer vision and pattern recognition*, 2016, pp. 770–778.

[14] J. Asanuma, S. Doi, and H. Igarashi, "Transfer learning through deep learning: application to topology optimization of electric motor," *IEEE Transactions on Magnetics*, vol. 56, no. 3, pp. 1–4, 2020.

[15] C. Gunnar, "Topology and data," *Bulletin of the American Mathematical Society*, vol. 46, no. 2, pp. 255–308, 2009.

[16] T. Qaiser, Y.-W. Tsang, D. Taniyama, N. Sakamoto, K. Nakane, D. Epstein, and N. Rajpoot, "Fast and accurate tumor segmentation of histology images using persistent homology and deep convolutional features," *Medical image analysis*, vol. 55, pp. 1–14, 2019.

[17] F. A. Khasawneh and E. Munch, "Chatter detection in turning using persistent homology," *Mechanical Systems and Signal Processing*, vol. 70, pp. 527–541, 2016.

[18] V. De Silva and R. Ghrist, "Coverage in sensor networks via persistent homology," *Algebraic & Geometric Topology*, vol. 7, no. 1, pp. 339–358, 2007.

[19] Y. Lee, S. D. Barthel, P. Dłotko, S. M. Moosavi, K. Hess, and B. Smit, "Quantifying similarity of pore-geometry in nanoporous materials," *Nature communications*, vol. 8, no. 1, pp. 1–8, 2017.

[20] Y. Hiraoka, T. Nakamura, A. Hirata, E. G. Escolar, K. Matsue, and Y. Nishiura, "Hierarchical structures of amorphous solids characterized by persistent homology," *Proceedings of the National Academy of Sciences*, vol. 113, no. 26, pp. 7035–7040, 2016. [Online]. Available: https://www.pnas.org/content/113/26/7035

[21] T. Aoyagi, Y. Otomo, H. Igarashi, H. Sasaki, Y. Hidaka, and H. Arita, "Prediction of current-dependent motor torque characteristics using deep learning for topology optimization," in *2021 23rd International Conference on the Computation of Electromagnetic Fields (COMPUMAG)*, 2022.

[22] H. Edelsbrunner, D. Letscher, and A. Zomorodian, "Topological persistence and simplification," in *Proceedings 41st annual symposium on foundations of computer science*. IEEE, 2000, pp. 454–463.

[23] A. Zomorodian and G. Carlsson, "Computing persistent homology," *Discrete & Computational Geometry*, vol. 33, no. 2, pp. 249–274, 2005.

[24] F. Chazal and B. Michel, "An introduction to topological data analysis: fundamental and practical aspects for data scientists," *arXiv preprint arXiv:1710.04019*, 2017.

[25] C. Tralie, N. Saul, and R. Bar-On, "Ripser.py: A lean persistent homology library for python," *The Journal of Open Source Software*, vol. 3, no. 29, p. 925, Sep 2018. [Online]. Available: https://doi.org/10.21105/joss.00925

[26] Y. Umeda, J. Kaneko, and H. Kikuchi, "Topological data analysis and its application to time-series data analysis," *Fujitsu Scientific & Technical Journal*, vol. 55, no. 2, pp. 65–71, 2019.

[27] K. He, X. Zhang, S. Ren, and J. Sun, "Deep residual learning for image recognition," in *Proceedings of the IEEE conference on computer vision and pattern recognition*, 2016, pp. 770–778.

VIII. BIOGRAPHIES

Bingnan Wang (M'12-SM'15) received his B.S. degree from Fudan University, Shanghai, China, in 2003, and Ph.D. degree from Iowa State University, Ames, IA, USA, in 2009, both in Physics. He has been with Mitsubishi Electric Research Laboratories (MERL), located in Cambridge, Massachusetts since then, and is now a Senior Principal Research Scientist. His research interests include electromagnetics and photonics, and their applications to wireless communications, wireless power transfer, sensing, electric machines, and energy systems.

AKM Khaled Ahsan Talukder is a PhD candidate in Computer Science and Engineering from Michigan State University, USA. He received B.Sc in Computer Science and Engineering from Rajshahi University of Engineering and Technology, Bangladesh in 2004 and received MEngSc in Computer Science and Software Engineering from The University of Melbourne, Australia in 2009. His research interests include multi-objective optimization algorithms, analysis of high-dimensional Pareto-optimal front and their applications in engineering design optimization and multi-criteria decision making.

Yusuke Sakamoto received B. Sc in 2009 and M. Sc degree in 2011, both from the University of Tokyo, Japan. He joined Mitsubishi Electric Corporation, Japan in 2011 and is currently engaged in research and development of electric motors. His special fields of interest include electric motors/actuators and charged particle accelerators. He is also a PhD candidate in Mechanical Engineering from Kyoto University, Japan.